Modifications in Chromatin Morphology and Organization During Sheep Oogenesis

VALENTINA RUSSO,[1*] ALESSANDRA MARTELLI,[1] PAOLO BERARDINELLI,[1] ORIANA DI GIACINTO,[1] NICOLA BERNABÒ,[1] DONATELLA FANTASIA,[2] MAURO MATTIOLI,[1] AND BARBARA BARBONI[1*]
[1]*Dipartimento di Scienze Biomediche Comparate, Università degli Studi di Teramo, 64100 Teramo, Italy*
[2]*Dipartimento di Scienze Biomediche, Sezione di Genetica Medica, Università di Chieti, 66100 Chieti, Italy*

KEY WORDS sheep; oocyte; nucleus; global DNA methylation; Dnmt1; telomeres; TERT

ABSTRACT This research has been designed to study the major events of nuclear remodeling that characterize sheep oocytes during the early stage of folliculogenesis (transition from preantral to antral stage). In particular, the modifications in large-scale chromatin configuration, the global DNA methylation, and the process of telomere elongation have been investigated as crucial events of oocyte nuclear maturity. In addition, the spatio-temporal distribution of the major enzymes involved in DNA methylation, the DNA methyltransferase 1 (Dnmt1), and in telomere elongation, telomerase catalytic subunit (TERT), have been described. To these aims, the nuclei of isolated oocytes were investigated using immunocytochemistry and Q-FISH analyses. In absence of preliminary information, these nuclear determinants were compared with those of fully competent germ cells obtained from medium and preovulatory antral follicles. The nuclei of sheep oocytes acquired a condensed chromatin configuration, stable high levels of global DNA methylation, and a definitive telomere length already in the majority of late growing stage oocytes (110 μm) derived from early antral follicles. In addition, while the process of methylation resulted strictly related to oocyte diameter, the telomeric program appeared to be highly chromatin configuration-dependent. The translocation of Dnmt1 and TERT from the nucleus to the cytoplasm in the oocytes derived from early antral follicles seems to confirm the definitive chromatin asset of these germ cells. In conclusion, changes in large-scale chromatin structure, epigenesis, and telomere size in the sheep are established prior to oocyte acquires the ability to resume meiosis. *Microsc. Res. Tech. 70:733–744, 2007.*

INTRODUCTION

After birth, mammalian ovaries are characterized by a defined pool of female gametes that dynamically grow increasing their diameter while the nuclei remain arrested in the first meiotic prophase. Physiologically, the oocytes become able to reinitiate the meiotic cell cycle at the end of this growing phase even if the process of meiotic maturation will start when, within preovulatory follicles, fully grown oocytes receive a positive stimulus represented by the gonadotropin surge.

Analogously, the fully grown germ cells are the only limited source of gametes for in vitro maturation and fertilization techniques even if the larger amount of oocytes is represented by the meiotic incompetent cells (Picton et al., 2003).

For this reason, many attempts have been made in rodents, sheep, bovines, and humans (Bao et al., 2003; Cecconi et al., 1999; Eppig and O'Brien, 1996; Van den Hurk et al., 2000; Yamamoto et al., 1999) to develop alternative in vitro approaches to use incompetent small oocytes isolated from primary and secondary follicles of untapped ovarian sources. The possibility of using the immature pool of oocytes continues to represent an attractive and crucial target in reproductive biotechnology for amplifying or conserving the genome of high value individuals even if, until now, the results in this contest are very limited.

Encouraging experiments (Bao et al., 2000, 2003) have recently been obtained showing that the nuclei isolated from mouse or bovine growing stage oocytes become competent to mature when transferred within the cytoplasm of fully grown germ cells supporting embryo process until term development. A new physiological concept derived from these experiments indicating that the nuclei of the oocytes reach the competence to sustain embryo development before the cytoplasm acquires the molecular machinery to drive maturation.

Nevertheless, to enhance this nuclear transfer procedure and to increase oocyte sources for an in vitro technique more information are required, in particular, information about the epigenetic status of the immature oocyte nucleus. In fact, one of the events that characterize gametogenesis is the epigenetic transformation of the genome required to regulate the future embryonic gene expression. In this contest, DNA methylation is one of the major epigenetic regulator of this process that interferes with gene expression and acts during the oogenesis as an important molecular mark underlying the parental-specific expression of genes subject

*Correspondence to: Dr. Valentina Russo or Prof. Barbara Barboni, Dipartimento di Scienze Biomediche Comparate, Piazza A. Moro 45, 64100 Teramo, Italy. E-mail: vrusso@unite.it or bbarboni@unite.it

Received 31 October 2006; accepted in revised form 6 February 2007

Contract grant sponsor: MIUR-PRIN 2004

DOI 10.1002/jemt.20462

Published online 29 March 2007 in Wiley InterScience (www.interscience.wiley.com).

to genomic imprinting (Lucifero et al., 2004; Reik and Walter, 2001a; Surani et al., 1984). Imprinted genes account for the complementary of both maternal and paternal genomes in normal development and play an essential role in regulating embryo growth, placental function, as well as in neurobehavioral processes (McGrath and Solter, 1984; Surani et al., 1984).

A number of genes regulated by imprinting contain differential methylation regions inherited from germ cells during gametogenesis (Geuns et al., 2003; Lucifero et al., 2002) as a consequence of the action of specific enzymes: the DNA methyltransferases (Dnmts), a family of de novo, and maintenance methylating enzymes responsible for the addition of the methyl group to the five-position of cytosine within CpG dinucleotids. The Dnmt isoforms involved in DNA methylation in the oocyte have yet to be identified (Swales and Spears, 2005), even if their role during oogenesis remains controversial. Some evidences, in human and mouse, have demonstrated that a spliced transcript of Dnmt1 protein (Dnmt1o) is found in the female germ cells and embryos (Dean et al., 2005; Mertineit et al., 1998; Swales and Spears, 2005). However, experiments performed on deficient mice for Dnmt1, Dnmt1o, and Dnmt3L display in all animals several loss of allele specific methylation expression of imprinted genes, implying a multiple contribution of the different isoforms in the process of germ cell methylation establishment and maintenance (Dean et al., 2005; Lucifero et al., 2004).

Recent evidence indicates that maternal methylation imprint establishment may be related to oocyte diameters as a consequence of the accumulation of these de novo methylating enzymes during the transition from primordial to antral follicles (Lucifero et al., 2004). Imprints seem to proceed in a gene specific manner and transform the DNA of fully grown oocytes in a highly methylated structure (Spinaci et al., 2004). Methylation is both a heritable and reversible epigenetic modification that is stably propagated after DNA replication and influences gene expression as does the process of chromatin condensation via the binding of several modulatory factors (Arney et al., 2001; Kono, 1998; Li, 2002). In fact, it is important to point out that the majority of DNA methylation in the genome is not concerned with genomic imprinting. Heavy methylation of DNA results in a more condensed structure, which is resistant to transcription (Swales and Spears, 2005).

Modifications in large-scale chromatin condensation during mammalian oocyte growth provide another important event that seems to coordinate the control of global transcription and defines the developmental potential of a germ cell (De La Fuente et al., 2004). In fact, chromatin in the oocyte nucleus (the germinal vesicle, GV) changes from a diffuse or decondensed configuration (nonsurrounded nucleolus, NSN), found predominantly in growing oocytes, and becomes progressively condensed around the nucleolus (surrounded nucleolus, SN) upon completion of oocyte growth (De La Fuente et al., 2004; Debey et al., 1993; Mattson and Albertini, 1990; Zuccotti et al., 1995). Importantly, the transition to the condensed configuration is temporally coordinated with global repression of transcription (Bouniol-Baly et al., 1999; De La Fuente and Eppig, 2001; De La Fuente et al., 2004).

Another fundamental biochemical prerequisite to define the developmental potential of a fully grown nucleus is the length of the telomeric structure (Keefe et al., 2005; Liu et al., 2002). Telomeres are specialized structures localized at the ends of eukaryotic chromosomes and are composed of conserved noncoding sequences of DNA repeats $(TTAGGG)_n$. These structures provide protection from enzymatic end-degradation and maintain chromosome stability during DNA replication. Recently, it has been reported that telomeres represent also an important prerequisite for the oocyte to express its developmental competence; in fact, telomere shortening in mouse and human oocytes triggers apoptosis in embryos (Keefe et al., 2005; Liu et al., 2002).

The enzyme involved in telomere rearrangement is telomerase, a ribonucleoprotein complex with reverse-transcriptase activity involved in telomere stability. It contains three major subunits: template RNA (TR), telomerase associated protein (TPI), and the reverse transcriptase subunit or telomerase catalytic subunit (TERT). The TERT component of telomerase is the primary determinant for enzyme activity and its expression is correlated to cells with telomere elongation (Cong et al., 1999; Misiti et al., 2000; Wang et al., 2000). Recently, TERT component has been related to the process of telomere rearrangement in pig germ cells during oogenesis where the presence of the enzyme within the nucleus has been strictly correlated to progressive telomere elongation (Russo et al., 2006).

Since the nuclear remodeling is a complicate mechanism that appears in part independent of the cytoplasm (Bao et al., 2000,2003), it appears extremely useful to improve the information about the exact timing and mechanisms involved in this process. In this context, the epigenetic dynamic and the telomeric rearrangement appear to be crucial determinants to deduce the developmental potential of oocytes. These elements remain still poorly and not systematically studied also in species, such as the ovine, that are largely used as animal model to develop knowledge and reproductive techniques (First, 1990; Peura and Vajta, 2003; Ritchie, 2006). Starting from this consideration, the present research was designed to characterize during the process of sheep oogenesis the female chromatin organization, in parallel with the spatio-temporal description of the major molecular determinants involved in epigenetic and telomeric program. In particular, the modifications in large-scale chromatin configuration have been analyzed in sheep growing oocytes and correlated to the epigenetic and telomeric configuration of their chromatin. In more detail, the process of epigenetic remodeling has been evaluated with immunocytochemistry analysis investigating the degree of global DNA methylation, while the status of telomere elongation has been detected with the FISH-processed section technique. Thus, to comprehend the contribution of the enzymatic machinery in the processes of nuclear rearrangement, the subcellular localization of Dnmt1 and TERT, respectively, these processes were evaluated at different stages of growing oocytes and fully grown oocytes.

MATERIALS AND METHODS

Tissue and Oocyte Collection

Ovaries were obtained during the breeding season from 2–4-year-old sheep of about 50 kg slaughtered at the local abattoir.

The ovaries, transported to the laboratory within 30 min, were trimmed of any extra tissue and preantral, early antral, and antral follicles were mechanically isolated as previously described (Cecconi et al., 1999). All the procedures were performed in dissection medium (Dulbecco's phosphate buffer medium with Ca^{2+} and Mg^{2+} supplemented with 0.4% BSA; Sigma), with the aid of a stereomicroscope.

After isolation, healthy follicles were chosen on the basis of their morphology. In particular, under the stereomiscroscope were considered the translucency of the follicle, the compactness of the follicular layers, the absence of free particles within antral cavity, and the presence of blood vessels (Cecconi et al., 1999; Mattioli et al., 2001).

Single healthy follicle diameters were, then, measured using an inverted-phase microscope equipped with an ocular micrometer (40× magnification) and classified as:

- small, and large preantral follicles (150 ± 40 μm and 250 ± 30 μm, respectively),
- early antral follicles (350 ± 50 μm), and
- medium antral follicles (~3 mm).

Each follicle was then carefully opened, and the released cumulus oocyte complex (COCs) was used in the following analyses which displayed a compact cumulus and an oocyte with homogeneous cytoplasm.

After removal of the cumulus cells, oocyte diameter was recorded before digesting the zonae pellucida according to Gioia et al. (2005). Zona-free oocytes were fixed in 4% paraformaldehyde/phosphate buffer saline for 1 h at 4°C, and then analyzed for GV chromatin configuration, global DNA methylation or Dnmt1, and TERT distribution.

To determine telomere size, using the fluorescence in situ hybridization (FISH) technique, the oocytes were processed within their follicle structures, according to Russo et al. (2006), dehydrated through ethanol series, and then embedded in paraffin wax.

Moreover, to compare the chromatin morphology of growing oocytes obtained from preantral and early antral follicles with that of fully grown and highly competent oocytes, preovulatory follicles (>6 mm) were isolated from 30 adult sheep. The animals were synchronized using a validated hormonal protocol (Lucidi et al., 2001; Willard et al., 2006). In detail, sponges of 30 mg flugestone acetate (Cronogest, Intervet; day 0) were intravaginally inserted for 12 days. One day before sponge removal, the animals were treated i.m. with 500 IU of equine chorionic gonadotropin (eCG; Folligon, Intervet) to prime follicular growth. The ovaries were surgically isolated 24 h after sponge removal by maintaining the animals under anesthesia with acepromazine maleate (0.05 mg/kg bodyweight) and pentothal sodium (10 mg/kg bodyweight). All protocols had prior approval of the Ethical Committee of the University of Teramo. The ovaries were then treated as described earlier.

Germinal Vesicle Chromatin Configuration

To classify the chromatin configuration, an aliquot of germ cells isolated from small and large preantral, early antral, medium, and preovulatory antral follicles were labeled for 30 min with 1 μM SYBR Green 14/I (Molecular Probes), one of the most sensitive stains available for detecting double-stranded DNA. The oocytes, washed in 0.05% Tween 20/PBS, were placed on glass slides, squashed with cover-slips, and analyzed with the laser scanning confocal microscope.

This chromatin configuration analysis was carried out on at least 40 germ cells of each follicle category, and on five oocytes isolated from preovulatory follicles.

Immunofluorescence Staining

Indirect immunofluorescence was carried out to evaluate and compare the degree of DNA methylation, the Dnmt1, and TERT subcellular localization in oocytes isolated from small and large preantral, early antral, medium, and preovulatory antral follicles.

After oocyte fixation, samples were washed in 0.05% Tween 20/PBS, and permeabilized with 0.2% Triton X100/0.05% Tween 20/PBS for 30 min at room temperature (RT).

The oocytes analyzed for global DNA methylation were treated in 2 M HCl for 30 min at RT to obtain DNA denaturation and then neutralized in 100 mM Tris HCl buffer (pH 8.5) for 10 min before primary antibody incubation.

Nonspecific binding was blocked by incubating the oocytes in normal goat serum (1:20 dilution; Sigma) for 1 h at RT. The primary antibody, a mouse anti-5-methylcytosine (Eurogentec), was maintained at the appropriate dilution (1:500 in PBS containing 1% BSA/0.05% Tween 20) overnight at 4°C. The oocytes, after extensive washing, were incubated with a goat antimouse Cy3 secondary antibody (1:400 in 0.05% Tween 20/PBS; Molecular Probes) for 1 h at RT and, finally, counterstained with 1 μM SYBR Green 14/I.

Immunocytochemistry for the DNA methyltransferase 1 (Dnmt1) was performed using a polyclonal goat antibody anti-Dnmt1 (Santa Cruz), specific for the C-terminal catalytic domain, which is highly conserved within all the Dnmt isoforms identified in female germ cells (Bestor, 2000). As described earlier, after blocking nonspecific bindings performed with the normal donkey serum (1:20 dilution; Sigma), the oocytes were incubated with the primary antibody diluted in PBS containing 1% BSA/0.05% Tween 20 (1:200), overnight at 4°C. Then, samples were washed in 0.05% Tween 20/PBS, exposed to a donkey antigoat Alexa Fluor488 conjugated antibody (Molecular Probes), and nuclear counterstaining was carried out with Propidium iodide (PI) 1 mg/mL (PI; Sigma) for 10 min at RT.

The cellular distribution of telomerase catalytic subunit was accomplished with a polyclonal rabbit antibody antireverse transcriptase (antihTERT, Calbiochem, Cui et al., 2002). After blocking nonspecific bindings with normal goat serum (1:20 dilution; Sigma), the primary antibody was applied overnight at 4°C (1:250 in PBS containing 1% BSA/0.05% Tween 20). A goat antirabbit conjugated Cy3 (Molecular Probes) was used as secondary antibody and chromatin was counterstained with 1 μM SYBR Green 14/I (Molecular Probes).

In all experiments, nonimmune serum was used in place of the primary antisera as negative control. All controls performed were negative.

Each immunofluorescence analysis was performed on at least 30 replicates (oocytes/follicular category), and on 10 oocytes isolated from preovulatory follicles.

Laser Confocal Microscopy and Quantitative Analysis

Observations were performed with a Bio-Rad laser scanning confocal microscope (Radiance 2000 IK-2), equipped with a krypton/argon ion laser. The sample were analyzed on an inverted microscope (Zeiss Axiovert) equipped with a plan-apochromat oil immersion objective 63× magnification/1.4 numerical aperture (NA). Immunostained and DNA-labeled oocytes were observed using the visible lines of excitation of 488 and 568 nm, and a dichroic filter (560LP, Bio-Rad). Digital optical sections were obtained by scanning the sample on *z*-axis at 0.2 μm of thickness throughout the plane of focus containing the GV equatorial plane (±20 μm). For each experiment, all the categories of oocytes were compared maintaining similar gain and laser parameters. The *z*-series were then projected to obtain a three-dimensional reconstruction and all the images were exported as eight bit-tagged image file format files.

When the degree of global DNA methylation was evaluated, according to Gioia et al. (2005), the *z*-series obtained were merged to produce a two-dimensional image showing the staining pattern and the total fluorescence intensity (TFI) emitted by each GV. The merged images were always corrected for the background represented by the mean intensity of the cytoplasmic area, and nuclear intensities were measured by manually outlining each GV. Then the TFI emitted from each GV was measured using the LaserPix software (Bio-Rad).

Fluorescence In Situ Hybridisation

Five-micron thick sections, obtained from paraffin embedded ovarian cortical pieces or isolated medium and preovulatory antral follicles were processed for FISH. Cross sections were deparaffinized by incubation for 10 min in xylene, washed for 10 min in 100% ethanol, and then air-dried. Slides were then placed in 2 × SSC at 45°C for 5 min., and subsequently treated with proteinase K (250 μg/mL; Sigma) in 2 × SSC at 45°C for 10 min. Slides were thoroughly rinsed with PBS, followed by dehydration in ethanol series (70, 95, and 100% at 2 min each), and air dried. Sections were denatured with 70% formamide (Carlo Erba) in 2 × SSC, pH 7.0 at 75.5°C for 5 min, followed immediately by dehydration in ice-cold ethanol (70, 95, and 100% at 2 min each), and allowed to air dry. A denatured all-human telomeric DNA probe was added to the slide (Qbiogene-Resnova) since eukaryotic chromosomes, as well as the sheep (de la Sena et al., 1995), contain conserved noncoding sequences of DNA repeats $(TTAGGG)_n$. Then, glass cover-slips were applied and sealed with rubber cement (Qbiogene-Resnova). After incubation overnight at 37°C in a humidified chamber, the slides were washed for 10 min in 50% formamide (Carlo Erba) in 2 × SSC at 37°C followed by washes at RT in 2 × SSC. The hybridized signals were detected by using a commercial kit [fluorescein isothiocyanate (FITC) avidin detection kit; Oncor] according to the manufacturer's instructions. PI/antifade 0.6 μg/mL (Qbiogene-Resnova) was used for chromatin counterstaining. All slides were analyzed using an Axioskop 2 Plus incident-light fluorescence microscope (Zeiss) equipped with a PL-Neofluorar × 100 oil immersion objective (NA 1.30) and a × 10 ocular to provide images with a spatial resolution of 0.25 μm, a HBO 100 W mercury lamp, a FITC/PI filter (excitation: 450–490; barrier: LP 520; no. 09, Zeiss), and a PI filter (excitation: BP 546; barrier: LP 590; no. 15, Zeiss). The microscope was also provided with a cooled color CCD camera (Axiovision Cam, Zeiss) with a resolution of 1300 × 1030 pixels, configured for fluorescence microscopy, and interfaced to a computer workstation, provided with an interactive and automatic image analyzer (Axiovision, Zeiss).

Q-FISH Analysis

Digital image analysis of telomere length was performed according to Miracco et al. (2002). For quantitative purposes, digital images were consecutively captured from sections immediately after hybridization with the fluoresceinated probes and counterstained with PI. Counterstain was used to scan the image and the FITC/PI filter was set to confirm the simultaneous presence of probe signals (green) and PI (red). At the beginning of an imaging session, optimum exposure times were determined and held constant thereafter. The oocyte nuclei (GV) were acquired by setting the luminous-field diaphragm on the whole area of the GV. This procedure was performed to exclude from the acquisition the fluorescent signals of granulosa cells. In all cases, it was confirmed that the telomeric signals were within the linear response range of the CCD camera, according to Meeker et al. (2002), using standard fluorescent microbeads (InSpeck microspheres; Molecular Probes). Image acquisition was performed with a dedicated software (Axiovision, Zeiss). After the acquisition of the digitized image, it was stored in a 1300 × 1030 pixels file. The images were imported in the 24-bit uncompressed TIF format, and then processed with the image analyzer, using the dedicated computer program (KS300 computed image analysis system, Zeiss). For the oocyte analysis, at least two cross sections, which included the nuclei of the oocytes, were considered for each germ cell. In more detail, 18 oocytes of small, and 20 of large preantral follicles, 23 oocytes of early antral follicles, 24 medium, and 10 preovulatory antral follicle oocytes were analyzed.

Quantification of the digitized fluorescent telomere signals was accomplished by using a semiautomated algorithm written with the image analysis software package KS300 (Zeiss). The computer program generates one image, showing the nuclei, which are stained red with PI, and the telomeres, which are assumed to hybridize quantitatively to the FITC fluorescent probe, and appear as bright green spots. After densitometric calibration of the background, the algorithm performs (i) segmentation of telomeres; (ii) measurements of their areas, lengths, and mean densitometric value; (iii) counts of number of telomeres per nuclear section. Briefly, after acquisition of the image, a geometric calibration is performed. A densitometric calibration follows, which relates the image to a 0–256 gray scale. Only the objects on the same planar focus are then chosen for the analysis. Parameters to be measured are then selected; these include number of telomeres,

mean densitometric value, area, and feret maximum, which corresponds to the value of the major diagonal connecting the two farthest points at the periphery of the object. Further background correction is then performed through Lowpass and Shadcorr filters. Segmentation of telomere spots is then improved; for each pixel, the average intensity value of neighboring pixels is subtracted from its intensity, resulting in a telomere pixel if the image of its edge is above a threshold level; otherwise, it is considered as a background or boundary pixel. Measures can be evaluated on the images of nuclei and telomeres by placing an electronic grid on them. Results are then recorded for statistical evaluation.

Statistical Analysis

All the data obtained from oocyte analyses at the different follicular stages were tested for normal distribution, and then compared using ANOVA (Microcal Origin 6.0). The data were expressed as mean ± standard deviation (SD). Statistical analyses were carried out on transformed data by logarithmic function; $P < 0.05$ was considered as significant and $P < 0.01$ were considered highly significant.

RESULTS

Oocyte Diameters and Chromatin Configurations

The mean diameter recorded in the oocytes isolated from small and large preantral follicles was 80 ± 5 and 90 ± 5 μm, respectively. Early antral follicles contained still growing oocytes with a diameter of 110 ± 10 μm, while a mean value of 120 ± 5 μm was recorded in fully grown germ cells obtained either from medium or preovulatory antral follicles.

GV chromatin configurations were revealed in sheep oocytes with SYBR Green 14/I staining and classified on the basis of the degree of condensation and distribution into three major categories: diffuse chromatin in the whole nuclear area (NSN), condensed chromatin surrounding the nucleolus (SN), and condensed chromatin near the nucleolus and the nuclear envelope (SNE).

The totality of the oocytes isolated from preantral follicles displayed a high dispersed chromatin in the nucleoplasm with a typical NSN configuration independently of the follicle diameter (Figs. 1A and 1B).

The SN pattern began to emerge in the 67% of germ cells isolated from early antral follicles while the remaining 33% maintained the NSN configuration (Fig. 1; C = NSN and D = SN), independently of their oocyte diameter (Fig. 2). In medium and preovulatory antral follicles, the germ cells displayed a high condensed chromatin that was distributed around the nucleolus and close to the nuclear envelope (SNE pattern; Fig. 1E).

Global DNA Methylation

The epigenetic remodeling has been evaluated studying the global DNA methylation using the 5-methylcytosine antibody and quantifying the TFI in the different categories of GVs.

The level of global methylation increased over the period of growth in relation to the process of follicle development. In fact, the absence of immunopositivity for the 5-methylcytosine antibody characterized the oocytes of small preantral follicles (Figs. 1F and 1K), while a faint degree of methylation started to appear in germ cells isolated from large preantral follicles (Figs. 1G and 1L).

The degree of DNA methylation increased in the oocytes isolated from early antral follicles, independently of the chromatin configuration recorded (Figs. 1H, 1I, 1M, and 1N). In addition, high levels of DNA methylation were observed in fully grown oocytes of medium (data not shown) and preovulatory antral follicles (Figs. 1J and 1O).

As shown in Figure 2, the quantitative analysis of the TFI emitted revealed that the degree of global DNA methylation was strictly dependent on oocyte diameter ($R^2 = 0.993$, obtained with the sigmoidal fitting of data; $P < 0.01$). In particular, the oocytes obtained from small preantral follicles (~80 μm) showed nondetectable values of TFI. The global DNA methylation progressively increased passing from the ~90 μm germ cells isolated from large preantral follicles up to the ~110 μm oocytes obtained from early antral follicles. Moreover, in the oocytes derived from early antral follicles the TFI value resulted independent of the chromatin configuration recorded ($P > 0.05$). TFI values remained stable in oocytes collected from medium and preovulatory antral follicles with a diameter of ~120 μm, as shown in Figure 2, indicating that the process of global DNA methylation is defined after antrum differentiation.

DNA Methyltranferase 1 (Dnmt1) Expression Pattern

The intracellular distribution of Dnmt1, a DNA methyltransferase involved in the maternal DNA methylation and maintenance, resulted strictly dependent on either the follicular stage considered or the oocyte diameter reached.

In fact, all growing oocytes isolated from small and large preantral follicles displayed a nuclear and cytoplasmic Dnmt1 localization (Fig. 3A). By contrast, the majority of germ cells isolated from early antral follicles (56%), independently of their chromatin configuration, showed the enzyme out of the nucleus in the cytoplasm (Fig. 3B). The cytoplasmatic distribution became prevalent in fully grown oocytes isolated from medium and preovulatory antral follicles where the enzyme was localized in the subcortical and the perinuclear region (Fig. 3C).

In Situ Analysis of Telomere Length (Q-FISH) in the Germinal Compartment

To study the relative size of single telomeres, FISH was performed on all the categories of germ cells considered.

In all the oocytes analyzed, telomeres were distributed in correspondence to the chromatin counterstained with PI (Fig. 4). The size of each hybridized telomere spot appeared to be independent of its distance by the nuclear periphery, indicating that individual differences in telomere-signal intensity within nuclei were not caused by local variations in probe access into the cell.

The oocytes of preantral follicles, independently of their stage (small or large), possessed a GV of about

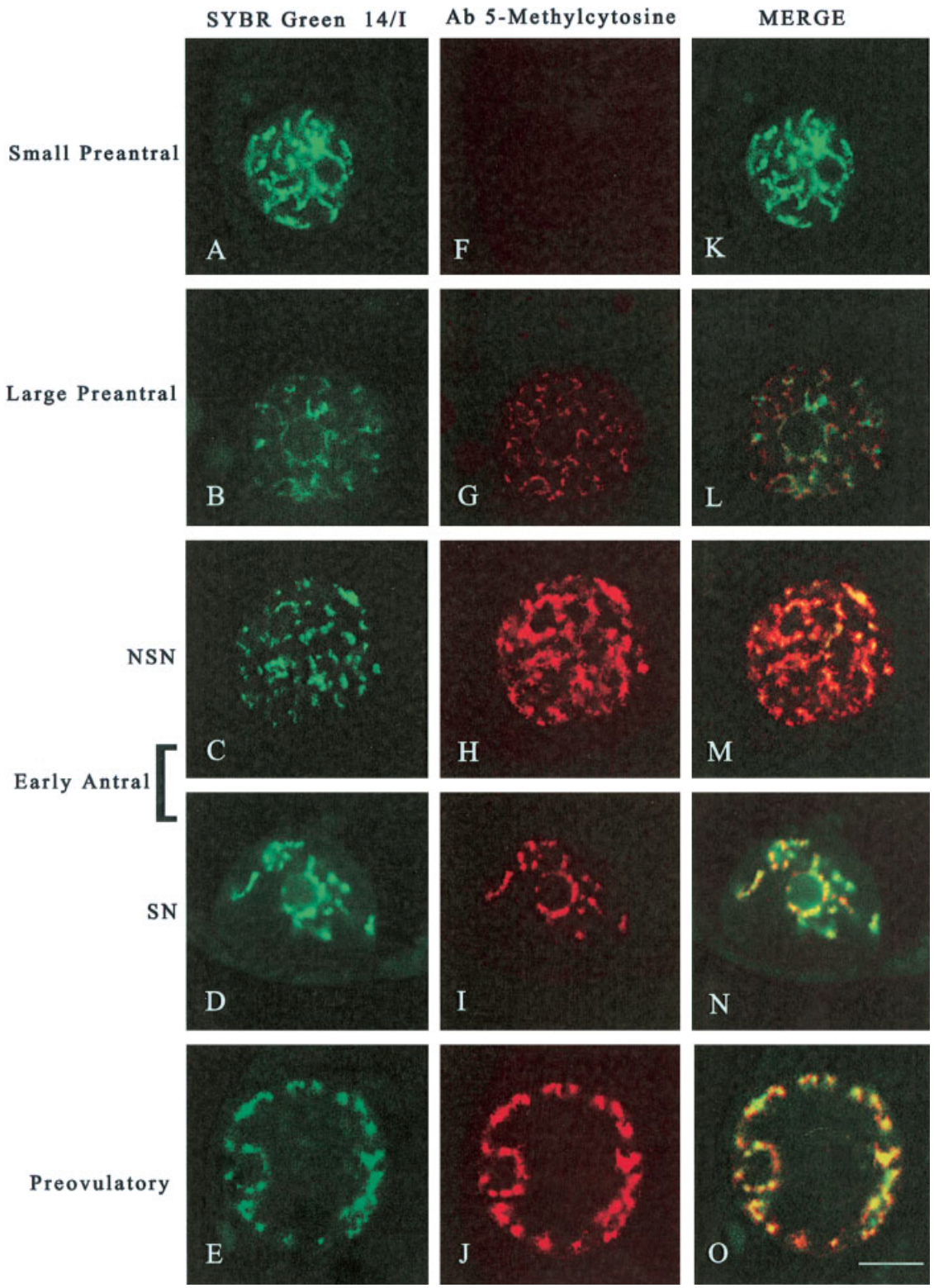

Fig. 1. Digital images of sheep GVs showing different chromatin configurations (left images), global DNA methylation patterns (middle images), and merged images (right images). Chromatin counterstaining was performed with SYBR Green 14/I (green), which detects double-stranded DNA, while global DNA methylation was analyzed with a 5-methylcytosine antibody (red). **A:** This picture shows a typical GV example of a germ cell obtained from a small preantral follicle with diffuse chromatin (NSN) that did not display any immunostaining for 5-methylcytosine (**F**, **K**). **B:** A GV example of an oocyte obtained from a large preantral follicle where the NSN chromatin started to display immunopositivity for 5-methylcytosine (**G**, **L**). The merged image on the right reveals that global DNA methylation staining resides exclusively with the SYBR Green 14/I staining. **C** and **D:** Two examples of oocytes obtained from early antral follicles with either a NSN chromatin or a SN configuration, respectively. In both categories of oocytes the 5-methylcytosine immunopositivity indicates the high degree of global DNA methylation (NSN = **H** and **M**, SN = **I** and **N**). **E:** GV of a fully grown oocyte isolated from a preovulatory follicle where the chromatin assumes the SNE pattern with a clear immunopositivity for 5-methylcytosine (**J**, **O**). Bar = 10 μm.

15–20 μm, showed a mean telomere number/section of 40.62 ± 3.10 and the following FISH values: telomere area (TEA) of 0.076 ± 0.045, a feret maximum (TEFmax) of 0.379 ± 0.124, and a mean densitometric value (MEAND) of 83.209 ± 27.168 (Fig. 5). Telomeric signals increased in germ cells of early antral follicles where similar mean telomere number/section was recorded within their GVs of ~20–25 μm in diameter (41.57 ± 4.63; $P > 0.05$). Although, only early antral oocytes with a SN configuration showed significantly bigger telomeres than those recorded in the oocytes enclosed in preantral follicles (SN oocytes: TEA 0.105 ± 0.079, $P < 0.01$; TEFmax 0.430 ± 0.175, $P < 0.01$; MEAND 110.911 ± 29.173, $P < 0.01$; Fig. 5). Instead, the oocytes with a NSN configuration, in terms of telomere size, were similar to the category of preantral follicle germ cells (TEA 0.071 ± 0.058, TEFmax 0.360 ± 0.147, MEAND 82.979 ± 18.331, $P > 0.05$; Fig. 5).

Oocytes derived from both categories of antral follicles showed similar telomere number and length values recorded in the SN oocytes isolated from early antral follicles. In detail, mean telomere number/section recorded within their GVs of ~25 μm in diameter was 41.5 ± 4.63 in medium antral follicles, and 40.9 ± 3.26 in preovulatory follicles ($P > 0.05$), while their telomere length values were TEA 0.104 ± 0.059; TEFmax 0.425 ± 0.154; MEAND 105.417 ± 22.293 for medium antral follicles, and TEA 0.106 ± 0.062; TEFmax 0.450 ± 0.151; MEAND 107.355 ± 20.299 for preovulatory follicles ($P > 0.05$; Fig. 5).

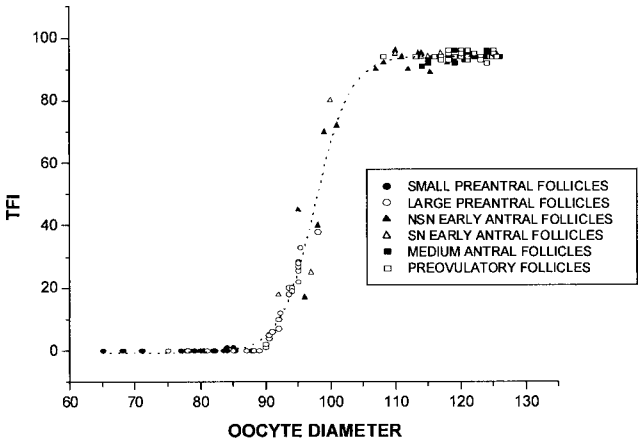

Fig. 2. Fitting of TFI values of global DNA methylation fluorescence with oocyte diameters recorded in germ cells obtained from small and large preantral, NSN and SN early antral, medium and preovulatory antral follicles ($R^2 = 0.993$, $P < 0.01$). The distribution curve revealed that global DNA methylation progressively increased from oocytes with a diameter of ~90 μm up to ~110 μm. The values of TFI did not change when the oocyte reached the fully grown stage (~120 μm in diameter).

TERT Expression Pattern

The telomerase catalytic subunit (TERT) was expressed in sheep oocytes, independently of the developmental stages considered, but its oocyte distribution was strictly dependent on follicle/oocyte growth.

The oocyte of small and large preantral follicles showed immunopositivity for TERT in the GV (Fig. 6A). By contrast, in early antral follicles, the oocytes started to localize TERT both in the nucleus and in the cytoplasm (71%, Fig. 6B). The remaining early antral oocytes displayed the protein localized within the nucleoplasm associated with a NSN chromatin configuration. Finally, in the germ cells of both categories of antral follicles TERT protein was exclusively ooplasmatic with, also in this case, a typical subcortical and perinuclear distribution (Fig. 6C).

DISCUSSION

Modifications in large-scale chromatin structure and DNA remodeling occur during specific phases of oocyte growth probably to organize the genome to attend embryo/fetal development (Arney et al., 2001; Kono, 1998; Zuccotti et al., 2005). Several evidences have demonstrated that chromatin organization (De La Fuente et al., 2004; Debey et al., 1993; Mattson and

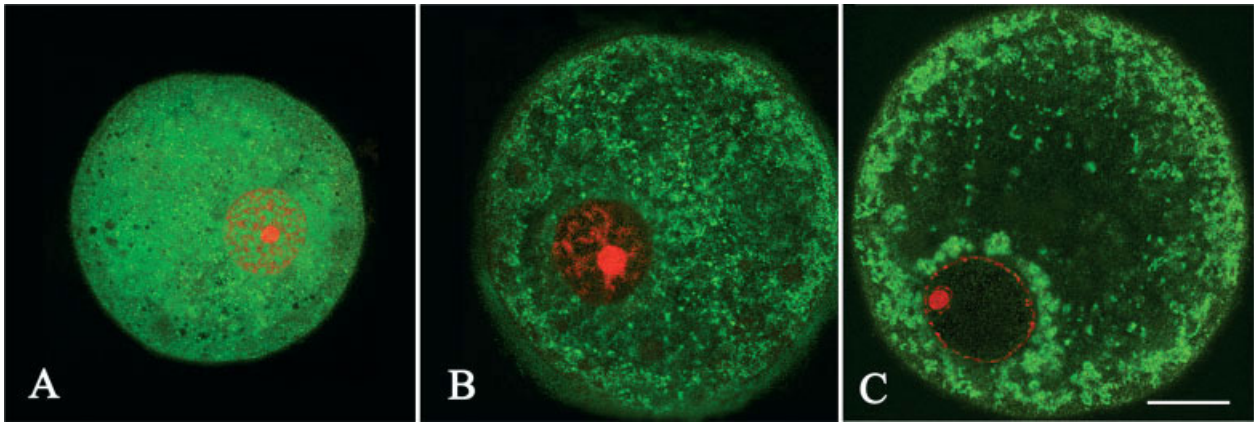

Fig. 3. Digital images showing Dnmt1 distribution during sheep oogenesis. Dnmt1 is visualized with Alexa Fluor488 secondary antibody (green), while DNA is counterstained with PI (red). **A:** An example of a growing oocyte obtained from a large preantral follicle which stained for Dnmt1 both in the nucleus and in the cytoplasm. The chromatin has a typical NSN configuration. **B:** Oocyte collected from an early antral follicle which displayed a cytoplasmic Dnmt1 staining that maintained a NSN chromatin configuration. **C:** An example of an oocyte obtained from a medium antral follicle where a clear subcortical and perinuclear ooplasmatic localization of the enzyme is recorded. The GV that did not show any positivity for the Dnmt1 antibody displayed a SNE chromatin configuration. Bar = 25 μm.

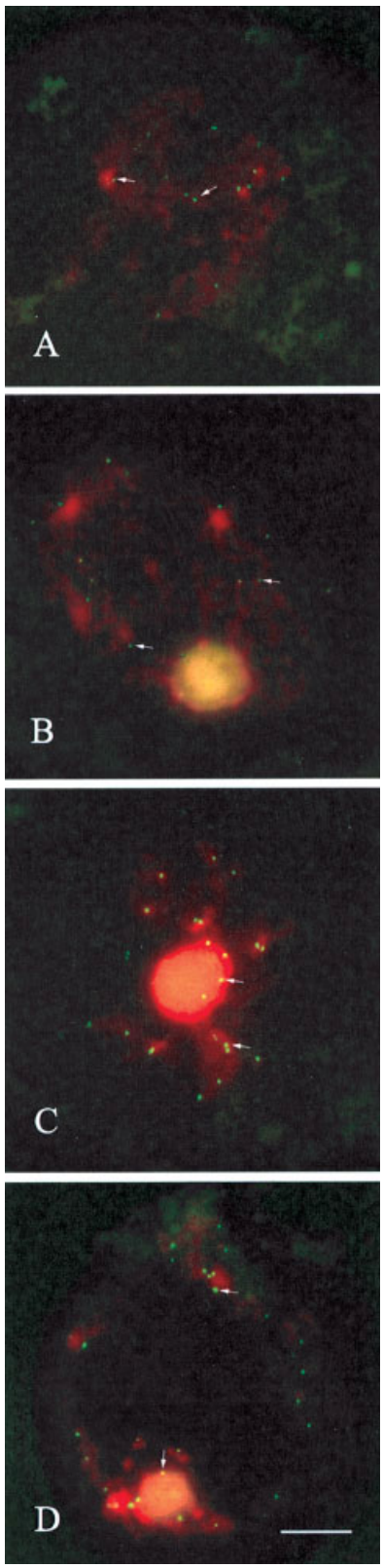

Albertini, 1990; Zuccotti et al., 1995), epigenetic status (Dean et al., 2005; Reik et al., 2001b; Swales and Spears, 2005), and telomeric size (Keefe et al., 2005, 2006; Liu et al., 2002) are crucial determinants to define the developmental competence of an oocyte even if information on the exact timing of these processes during oogenesis remains largely unknown.

Therefore, the molecular characterization of the oocyte chromatin may represent an important tool to predict the competence of a female germ cell as well as to identify the causes of the developmental anomalies revealed during the application of several assisted reproductive technologies that, as a consequence of an altered expression of imprinted genes, have been related to diseases during the postnatal life as the large offspring syndrome in sheep and cow (Lazzari et al., 2002; Young et al., 2001).

Starting from this consideration and in the absence of any preliminary information, this study has been addressed to compare the nucleus of sheep growing oocytes with that of fully competent grown oocytes collected from preovulatory follicles to determine at which follicular stage or oocyte diameter the germ cell acquires a mature chromatin organization.

This research demonstrates that the majority of the germ cells of 110 μm displayed a definitive degree of chromatin condensation, global DNA methylation, and telomere elongation in advance with respect to the acquisition of a biochemical machinery able to drive the resumption of meiosis. In fact, only sheep oocytes derived from antral follicles of ~2 mm in diameter of adult ovaries can progress in meiosis in high percentage and 70% of total oocytes reach metaphase II (Ledda et al., 1999; Moor and Tounson, 1997).

For these nuclear parameters, a whole remodeling seems to be coincident with the process of follicle antrum differentiation. In fact, during the transition from preantral to early antral follicles, the GV assumes a nuclear organization similar to that of the fully grown oocytes isolated from preovulatory follicles.

In particular, the analysis of the GV showed a progressive organization of large-scale chromatin configuration during sheep oocyte growth. In fact, a diffuse chromatin throughout the nucleus (NSN pattern) characterized all immature oocytes isolated from sheep preantral follicles independently of their diameter, according to that observed in other species such as mouse, pig, goat, and

Fig. 4. Examples of digital images of GV telomeres analyzed in oocytes enclosed within preantral, early antral, and antral follicles using the Q-FISH technique. In these paraffin-embedded tissue sections, telomeres are visualized as bright green spots (FITC) while DNA is counterstained in red with PI. In addition, the GVs were acquired by closing the luminous-field diaphragm until the entire nuclei was visible in the field of view. In all the digital images telomeres (arrows) are distributed in correspondence to the chromatin. Examples of (**A**) nucleus located within an oocyte derived from a large preantral follicle showing a NSN chromatin configuration and the relative telomeres, (**B**) GVs of early antral follicle oocytes with a NSN, or (**C**) with a SN configuration. In the images it can be qualitatively appreciated the higher fluorescence signal emitted from the telomeres of the GV with the SN chromatin configuration in comparison to those recorded within the NSN one, (**D**) Nucleus of a fully grown oocyte derived from a medium antral follicle. In this microphotograph, telomeres can be appreciated close to the chromatin condensed around the nucleolus and the nuclear membrane. Scale bars = 5 μm.

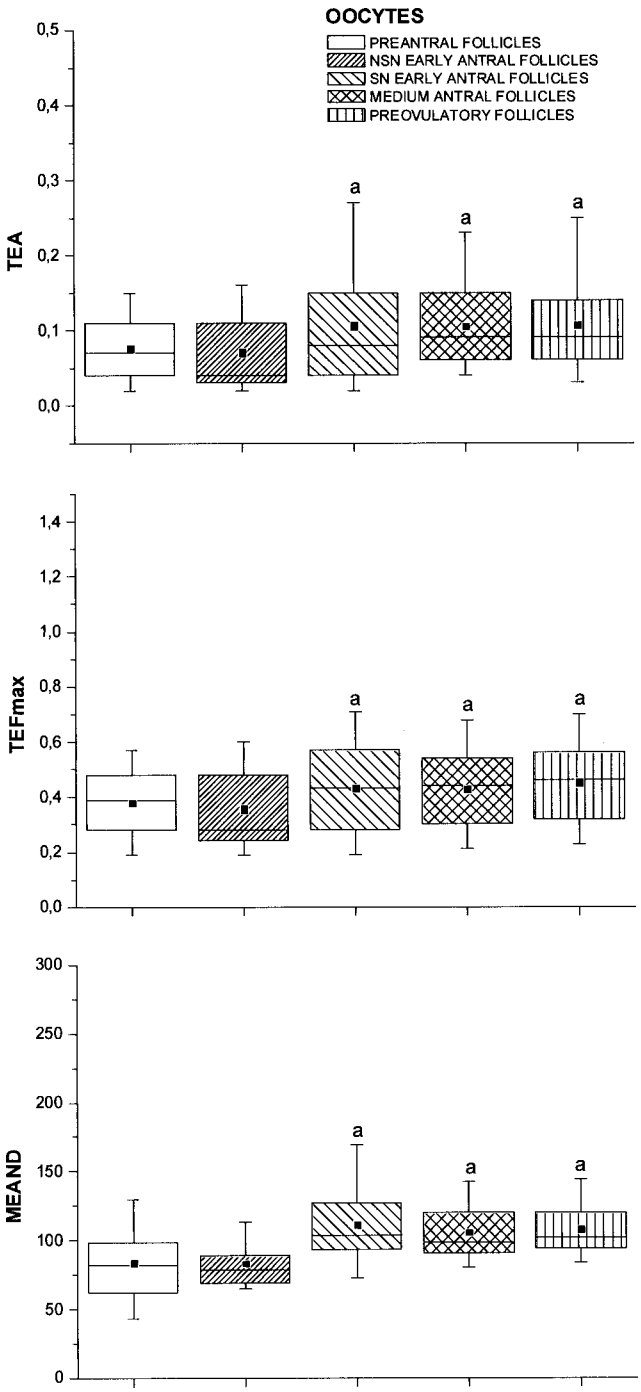

Fig. 5. Telomere area (TEA), feret maximum (TEFmax), and mean densitometric value (MEAND) examined in the GVs of large preantral, NSN and SN early antral, medium and preovulatory antral follicles. The horizontal lines in the box plots express the 5th, 25th, 50th, 75th, and 95th percentile of the distribution. The box stretches from the 25th to the 75th percentile, and therefore contains the middle half of the scores in the distribution. The median is shown as a line across the box, meanwhile the mean value as a black square within the box. The data of TEA, TEFmax, and MEAND that resulted highly significantly different ($P < 0.01$) after statistical analysis were indicated by the superscript a.

bovine (Sun et al., 2004; Zuccotti et al., 1995; bovine: Liu et al., 2006; goat: Sui et al., 2005; mouse: Mattson and Albertini, 1990; pig: Guthrie and Garret, 2000).

Analogously, to the mice model, the NSN seems to be an immature chromatin configuration that the oocytes loose when they gain the full meiotic competence (Zuccotti et al., 1995).

In fact, along with the growing phase, a condensed chromatin surrounding the nucleolus (SN pattern) started to appear and characterized sheep oocytes of 110 ± 10 μm isolated from early antral stage follicles. However, differently to the mouse, the SN configuration did not represent the more advanced configuration toward ovulation, since medium and preovulatory antral follicles developed a new pattern of GV organization where the condensed chromatin appeared localized partly around the nucleolus and partly close to the nuclear envelope (SNE pattern). Recently, similar observations were reported from Liu et al. (2006) in bovine fully grown oocytes before GVBD suggesting that the ruminants have more in common with each other than with different mammalian species (mouse, pig).

Many reports linked a highly condensed chromatin to an inactive transcriptional form of chromatin that precedes the meiotic competence (De La Fuente, 2006; Liu et al., 2006; Zuccotti et al., 2005). A growing body of evidence indicates that the chromatin structure together with DNA methylation mutually reinforce the transcriptionally repressive states of DNA (Fuks et al., 2003; Tamaru and Selker, 2001).

In this contest, over the period of growth, the global degree of DNA methylation in the oocyte progressively increases as both the appropriate maternal pattern is laid down and nonimprinted sequences become methylated. The process of DNA methylation on single female germ cells has not been examined yet, but information on the timing of the process, at least for a number of imprinted sex-specific genes, are available in the mouse (Allegrucci et al., 2005) where the methylation marks have been described during postnatal life on a population of germ cells of known developmental stage (Dean et al., 2005; Lucifero et al., 2004).

In this research, analyzing directly single germ cells, it was possible to follow the global DNA methylation over the period of germ cell growth and to correlate the epigenetic status with the processes of follicle and oocyte development.

In the sheep, an intense process of global DNA methylation involved physiologically the germinal cells of large preantral follicles that stabilize in the oocytes isolated from tertiary antral follicles, independently of the stage of development. Surprisingly, both chromatin configurations (NSN and SN) visualized in the oocytes obtained from early antral follicles showed similar TFI values of 5-methylcytosine antibody suggesting that the degree of global DNA methylation is not temporally related to the condensation of chromatin configuration. Instead, the major epigenetic regulatory process seems to be influenced by the oocyte diameter. In fact, the germ cells that reached a diameter of at least 110 μm displayed a high and stable degree of global DNA methylation expressed as TFI for the 5-methylcytosine antibody. It must be stressed that when the oocyte reached a definitive global DNA methylation, this biochemical modification of the DNA in the oocyte is maintained until fertilization, differently from other epigenetic processes that continue to operate during the matura-

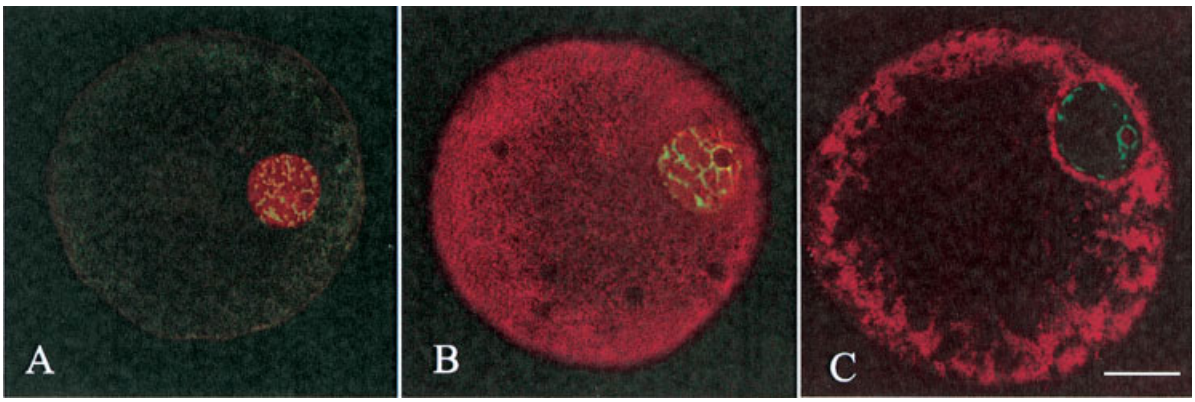

Fig. 6. Microphotographs showing immunocytochemistry analysis for the telomerase catalytic subunit (TERT) in preantral, early antral, and antral follicle oocytes. In these images TERT is visualized with an antirabbit secondary antibody conjugated Cy3 (red), while DNA is counterstained in green with SYBR Green 14/I. **A:** An example of a large preantral follicle oocyte which localizes TERT in the nucleus. **B:** Oocyte derived from an early antral follicle which reveals TERT distributed either in the nucleus, where is evident a SN chromatin configuration, or in the ooplasm. **C:** An example of an oocyte of a preovulatory antral follicle, which shows a clear subcortical and perinuclear cytoplasmatic TERT distribution. Scale bar = 25 μm.

tion window as the acetylase/deacetylase balance that is strictly cell-cycle dependent (Spinaci et al., 2004).

Several studies suggest a mutual interrelatedness of the different isoforms of Dnmts to create and maintain distinctive patterns and levels of DNA methylation that define specific genomic regions (Dean et al., 2005; Lucifero et al., 2004).

As regards the mammalian oocyte, the Dnmt involved in the epigenetic process during the growing phase has to be identified yet (Swales and Spears, 2005). The Dnmt1, and in particular, a spliced transcript of Dnmt1 protein (Dnmt1o) is actively transcribed and translated during oocyte growth and maturation or in preimplantation embryos (Dean et al., 2005; Mertineit et al., 1998; Swales and Spears, 2005). Moreover, Dnmt1 has been shown to be associated with a wide variety of chromatin modifying activities, including histone methyltranferases, methyl CpG binding proteins, and heterochromatin binding protein HP1 (Hermann et al., 2004). Collectively, these associations share in common the properties of transcriptional repressors leading to the understanding that Dnmt1 and, hence, DNA methylation stably reinforces chromatin silencing (Bird, 2002), and contributes to the preservation of the correct organization of large heterochromatic regions (Espada et al., 2004). In this research, the localization of Dnmt1 in sheep oocytes during the oogenesis in the postnatal life has been described. In summary, Dnmt1 is operative in germ cells of preantral follicles where a clear nuclear distribution of the enzyme has been recorded. By contrast, the Dnmt1 in early antral follicle oocytes started to translocate from the nucleus to the ooplasm assuming in germ cells of medium and preovulatory antral follicles a typical subcortical and perinuclear distribution.

The morphological evidence that Dnmt1 is exported from the nucleus to the cytoplasm in late growing oocytes involves, as a functional consequence, the inactivity of the enzyme and may indirectly confirm the end of the DNA methylating process.

The Dnmt1 cytoplasmic translocation has been previously described in the mouse growing germ cells (Mertineit et al., 1998), although this event occurred earlier, probably due to the faster oogenesis in this animal model in comparison with farm animals. Moreover, it must be pointed out that the Dnmt1 distribution pattern appears to be temporally associated with the process of global DNA methylation, but neither Dnmt1 ooplasmic translocation or the high degree of DNA methylation correspond to the acquisition of a condensed chromatin.

Another crucial requisite that defines the developmental potential of mouse and human fully grown oocytes is the length of telomeres (Keefe et al., 2005, 2006; Liu et al., 2002). This research, with the aid of the Q-FISH technique which permits the assessment of telomere size on tissue sections from standard formalin fixed paraffin-embedded samples (Meeker et al., 2002; Miracco et al., 2002; Russo et al., 2006; Tanemura et al., 2005), highlights that telomeres are actively rearranged during sheep oocyte growth. In particular, telomere elongation proceeds in germ cells from preantral to early antral follicles and stabilizes after antrum differentiation. Interestingly, telomere elongation was observed in the oocytes isolated from the follicular stage in which TERT was exactly localized in the germinal vesicle. Although, it is important to notice that telomere elongation in early antral follicle oocytes is strictly chromatin configuration dependent. In fact, the same telomere length values were recorded in NSN oocytes enclosed both in preantral and early antral follicles. Instead, where the active chromatin remodeling is concluded, TERT expression stops in the nucleus and starts to be localized in the ooplasm, and significantly longer and stable telomeres characterize the SN growing oocytes from early antral and the SNE fully grown germ cells derived from antral follicles. In these germ cells, a clear nonfunctional cytosolic TERT distribution was always recorded. The telomere elongation demonstrated during the transition from preantral to early antral follicles seems to be an important process in the female germ cells since telomere length might serve in the zygote after fertilization as a zero-time length mark for the subsequent embryo cell divisions. In fact,

it has been demonstrated that fertilized eggs from late generations of telomerase-null ($TR^{-/-}$) mice exhibited a high incidence of apoptosis, as evidenced by both cytofragmentation and nuclear DNA fragmentation (Liu et al., 2002). More recently, Keefe et al. (2005) demonstrated that telomere length predicts cytoplasmic fragmentation in embryos from women undergoing IVF for treatment of infertility, in fact telomere shortening in human oocytes triggers apoptosis in embryos. Since it has been demonstrated that telomere length predicts cytoplasmic fragmentation in embryos, a detailed understanding of the telomere-elongation program could be important for studying oocyte quality providing a useful predictor of outcome after IVF treatment. Furthermore, the location of TERT in the subcortical and perinuclear region of germ cells from medium and preovulatory antral follicles, such as Dnmt1, reproduces the behavior of other different maternal stock of quiescent proteins that will help the oocyte after fertilization until the activation of the embryonic genome.

In conclusion, in sheep germ cells, a definitive nuclear configuration in terms of chromatin condensation, global DNA methylation, and telomere elongation is acquired already in late growing stage oocytes (110 μm) when the follicle showed a differentiated antrum. This study carried out analytically on single germ cells demonstrated that the changes in large-scale chromatin structure precedes the development to the full size and, for this reason, occurs in advance with respect to the acquisition of the ability of the oocyte to resume meiosis.

This evidence strengthens the idea that growing oocytes can represent an early source of maternal genome by adopting a nuclear transfer approach, as demonstrated earlier empirically in the mouse and bovine (Bao et al., 2000, 2003). In addition, the kinetic definition of the nuclear events during oogenesis opens the possibility to adopt new chromatin marks to evaluate germ cells used or obtained by using different in vitro assisted technologies as in vitro folliculogenesis, in vitro oocyte maturation, and fertilization.

ACKNOWLEDGMENTS

The authors thank Terenzio Fabbroni, Zeiss advisor, for his technical assistance with KS300 computed image analysis system.

REFERENCES

Allegrucci C, Thurston A, Lucas E, Young L. 2005. Epigenetics and the germline. Reproduction 129:137–149.

Arney KL, Erhardt S, Drewell RA, Surani MA. 2001. Epigenetic reprogramming of the genome—From the germ line to the embryo and back again. Int J Dev Biol 45:533–540.

Bao S, Obata Y, Carroll J, Domeki I, Kono T. 2000. Epigenetic modifications necessary for normal development are established during oocyte growth in mice. Biol Reprod 62:616–621.

Bao S, Ushijima H, Hirose A, Aono F, Ono Y, Kono T. 2003. Development of bovine oocytes reconstructed with a nucleus from growing stage oocytes after fertilization in vitro. Theriogenology 59:1231–1239.

Bestor TH. 2000. The DNA methyltransferases of mammals. Hum Mol Genet 9:2395–2402.

Bird A. 2002. DNA methylation patterns and epigenetic memory. Genes Dev 16:6–21.

Bouniol-Baly C, Hamraoui L, Guibert J, Beaujean N, Szollosi MS, Debey P. 1999. Differential transcriptional activity associated with chromatin configuration in fully grown mouse germinal vesicle oocytes. Biol Reprod 60:580–587.

Cecconi S, Barboni B, Coccia M, Mattioli M. 1999. In vitro development of sheep preantral follicles. Biol Reprod 60:594–601.

Cong YS, Wen J, Bacchetti S. 1999. The human telomerase catalytic subunit hTERT: Organization of the gene and characterization of the promoter. Hum Mol Genet 8:137–142.

Cui W, Aslam S, Fletcher J, Wylie D, Clinton M, Clark AJ. 2002. Stabilization of telomere length and karyotypic stability are directly correlated with the level of hTERT gene expression in primary fibroblasts. J Biol Chem 277:38531–38539.

De La Fuente R. 2006. Chromatin modifications in the germinal vesicle (GV) of mammalian oocytes. Dev Biol 292:1–12.

De La Fuente R, Eppig JJ. 2001. Transcriptional activity of the mouse oocyte genome: Companion granulosa cells modulate transcription and chromatin remodeling. Dev Biol 229:224–236.

De La Fuente R, Viveiros MM, Burns KH, Adashi EY, Matzuk MM, Eppig JJ. 2004. Major chromatin remodeling in the germinal vesicle (GV) of mammalian oocytes is dispensable for global transcriptional silencing but required for centromeric heterochromatin function. Dev Biol 275:447–458.

de la Sena C, Chowdhary BP, Gustavsson I. 1995. Localization of the telomeric (TTAGGG)n sequences in chromosomes of some domestic animals by fluorescence in situ hybridization. Hereditas 123:269–274.

Dean W, Lucifero D, Santos F. 2005. DNA methylation in mammalian development and disease. Birth Defects Res C Embryo Today 75: 98–111.

Debey P, Szollosi MS, Szollosi D, Vautier D, Girousse A, Besombes D. 1993. Competent mouse oocytes isolated from antral follicles exhibit different chromatin organization and follow different maturation dynamics. Mol Reprod Dev 36:59–74.

Eppig JJ, O'Brien MJ. 1996. Development in vitro of mouse oocytes from primordial follicles. Biol Reprod 54:197–207.

Espada J, Ballestar E, Fraga MF, Villar-Garea A, Juarranz A, Stockert JC, Robertson KD, Fuks F, Esteller M. 2004. Human DNA methyltransferase 1 is required for maintenance of the histone H3 modification pattern. J Biol Chem 279:37175–37184.

First NL. 1990. New animal breeding techniques and their application. J Reprod Fertil Suppl 41:3–14.

Fuks F, Hurd PJ, Wolf D, Nan X, Bird AP, Kouzarides T. 2003. The methyl-CpG-binding protein MeCP2 links DNA methylation to histone methylation. J Biol Chem 278:4035–4040.

Geuns E, De Rycke M, Van Steirteghem A, Liebaers I. 2003. Methylation imprints of the imprint control region of the SNRPN-gene in human gametes and preimplantation embryos. Hum Mol Genet 12:2873–2879.

Gioia L, Barboni B, Turriani M, Capacchietti G, Pistilli MG, Berardinelli P, Mattioli M. 2005. The capability of reprogramming the male chromatin after fertilization is dependent on the quality of oocyte maturation. Reproduction 130:29–39.

Guthrie HD, Garrett WM. 2000. Changes in porcine oocyte germinal vesicle development as follicles approach preovulatory maturity. Theriogenology 54:389–399.

Hermann A, Gowher H, Jeltsch A. 2004. Biochemistry and biology of mammalian DNA methyltransferases. Cell Mol Life Sci 61:2571–2587.

Keefe DL, Franco S, Liu L, Trimarchi J, Cao B, Weitzen S, Agarwal S, Blasco MA. 2005. Telomere length predicts embryo fragmentation after in vitro fertilization in women—Toward a telomere theory of reproductive aging in women. Am J Obstet Gynecol 192:1256–1260.

Keefe DL, Marquard K, Liu L. 2006. The telomere theory of reproductive senescence in women. Curr Opin Obstet Gynecol 18:280–285.

Kono T. 1998. Influence of epigenetic changes during oocyte growth on nuclear reprogramming after nuclear transfer. Reprod Fertil Dev 10:593–598.

Lazzari G, Wrenzycki C, Herrmann D, Duchi R, Kruip T, Niemann H, Galli C. 2002. Cellular and molecular deviations in bovine in vitro-produced embryos are related to the large offspring syndrome. Biol Reprod 67:767–775.

Ledda S, Bogliolo L, Leoni G, Naitana S. 1999. Follicular size affects the meiotic competence of in vitro matured prepubertal and adult oocytes in sheep. Reprod Nutr Dev 39:503–508.

Li E. 2002. Chromatin modification and epigenetic reprogramming in mammalian development. Nat Rev Genet 3:662–673.

Liu L, Blasco M, Trimarchi J, Keefe D. 2002. An essential role for functional telomeres in mouse germ cells during fertilization and early development. Dev Biol 249:74–84.

Liu Y, Sui HS, Wang HL, Yuan JH, Luo MJ, Xia P, Tan JH. 2006. Germinal vesicle chromatin configurations of bovine oocytes. Microsc Res Tech 69:799–807.

Lucidi P, Barboni B, Mattioli M. 2001. Ram-induced ovulation to improve artificial insemination efficiency with frozen semen in sheep. Theriogenology 55:1797–1805.

Lucifero D, Mertineit C, Clarke HJ, Bestor TH, Trasler JM. 2002. Methylation dynamics of imprinted genes in mouse germ cells. Genomics 79:530–538.
Lucifero D, Mann MR, Bartolomei MS, Trasler JM. 2004. Gene-specific timing and epigenetic memory in oocyte imprinting. Hum Mol Genet 13:839–849.
Mattioli M, Barboni B, Turriani M, Galeati G, Zannoni A, Castellani G, Berardinelli P, Scapolo PA. 2001. Follicle activation involves vascular endothelial growth factor production and increased blood vessel extension. Biol Reprod 65:1014–1019.
Mattson BA, Albertini DF. 1990. Oogenesis: Chromatin and microtubule dynamics during meiotic prophase. Mol Reprod Dev 25:374–383.
McGrath J, Solter D. 1984. Completion of mouse embryogenesis requires both the maternal and paternal genomes. Cell 37:179–183.
Meeker AK, Gage WR, Hicks JL, Simon I, Coffman JR, Platz EA, March GE, De Marzo AM. 2002. Telomere length assessment in human archival tissues: Combined telomere fluorescence in situ hybridization and immunostaining. Am J Pathol 160:1259–1268.
Mertineit C, Yoder JA, Taketo T, Laird DW, Trasler JM, Bestor TH. 1998. Sex-specific exons control DNA methyltransferase in mammalian germ cells. Development 125:889–897.
Miracco C, De Santi M, Schurfeld K, Santopietro R, Lalinga AV, Fimiani M, Biagioli M, Brogi M, De Felice C, Luzi P, Andreassi L. 2002. Quantitative in situ evaluation of telomeres in fluorescence in situ hybridization-processed sections of cutaneous melanocytic lesions and correlation with telomerase activity. Br J Dermatol 146:399–408.
Misiti S, Nanni S, Fontemaggi G, Cong YS, Wen J, Hirte HW, Piaggio G, Sacchi A, Pontecorvi A, Bacchetti S, Farsetti A. 2000. Induction of hTERT expression and telomerase activity by estrogens in human ovary epithelium cells. Mol Cell Biol 20:3764–3771.
Moor RM, Trounson AO. 1977. Hormonal and follicular factors affecting maturation of sheep oocytes in vitro and their subsequent developmental capacity. J Reprod Fertil 49:101–109.
Peura TT, Vajta G. 2003. A comparison of established and new approaches in ovine and bovine nuclear transfer. Cloning Stem Cells 5:257–277.
Picton HM, Danfour MA, Harris SE, Chambers EL, Huntriss J. 2003. Growth and maturation of oocytes in vitro. Reprod Suppl 61:445–462.
Reik W, Walter J. 2001a. Genomic imprinting: Parental influence on the genome. Nat Rev Genet 2:21–32.
Reik W, Dean W, Walter J. 2001b. Epigenetic reprogramming in mammalian development. Science 293:1089–1093.
Ritchie WA. 2006. Nuclear transfer in sheep. Methods Mol Biol 325:11–23.
Russo V, Berardinelli P, Martelli A, Di Giacinto O, Nardinocchi D, Fantasia D, Barboni B. 2006. Expression of telomerase reverse transcriptase subunit (TERT) and telomere sizing in pig ovarian follicles. J Histochem Cytochem 54:443–455.
Spinaci M, Seren E, Mattioli M. 2004. Maternal chromatin remodeling during maturation and after fertilization in mouse oocytes. Mol Reprod Dev 69:215–221.
Sui HS, Liu Y, Miao DQ, Yuan JH, Qiao TW, Luo MJ, Tan JH. 2005. Configurations of germinal vesicle (GV) chromatin in the goat differ from those of other species. Mol Reprod Dev 71:227–236.
Sun XS, Liu Y, Yue KZ, Ma SF, Tan JH. 2004. Changes in germinal vesicle (GV) chromatin configurations during growth and maturation of porcine oocytes. Mol Reprod Dev 69:228–234.
Surani MA, Barton SC, Norris ML. 1984. Development of reconstituted mouse eggs suggests imprinting of the genome during gametogenesis. Nature 308:548–550.
Swales AK, Spears N. 2005. Genomic imprinting and reproduction. Reproduction 130:389–399.
Tamaru H, Selker EU. 2001. A histone H3 methyltransferase controls DNA methylation in Neurospora crassa. Nature 414:277–283.
Tanemura K, Ogura A, Cheong C, Gotoh H, Matsumoto K, Sato E, Hayashi Y, Lee HW, Kondo T. 2005. Dynamic rearrangement of telomeres during spermatogenesis in mice. Dev Biol 281:196–207.
Van den Hurk R, Abir R, Telfer EE, Bevers MM. 2000. Primate and bovine immature oocytes and follicles as sources of fertilizable oocytes. Hum Reprod Update 6:457–474.
Wang Z, Kyo S, Takakura M, Tanaka M, Yatabe N, Maida Y, Fujiwara M, Hayakawa J, Ohmichi M, Koike K, Inoue M. 2000. Progesterone regulates human telomerase reverse transcriptase gene expression via activation of mitogen-activated protein kinase signaling pathway. Cancer Res 60:5376–5381.
Willard ST, Dickerson T, Dodson R, Weis A, Godfrey RW. 2006. Administration of 6-methoxybenzoxazolinone (MBOA) does not augment ovulatory responses in St. Croix White ewes superovulated with PMSG. Anim Reprod Sci 93:280–291.
Yamamoto K, Otoi T, Koyama N, Horikita N, Tachikawa S, Miyano T. 1999. Development to live young from bovine small oocytes after growth, maturation and fertilization in vitro. Theriogenology 52:81–89.
Young LE, Fernandes K, McEvoy TG, Butterwith SC, Gutierrez CG, Carolan C, Broadbent PJ, Robinson JJ, Wilmut I, Sinclair KD. 2001. Epigenetic change in IGF2R is associated with fetal overgrowth after sheep embryo culture. Nat Genet 27:153–154.
Zuccotti M, Piccinelli A, Giorgi Rossi P, Garagna S, Redi CA. 1995. Chromatin organization during mouse oocyte growth. Mol Reprod Dev 41:479–485.
Zuccotti M, Garagna S, Merico V, Monti M, Alberto Redi C. 2005. Chromatin organisation and nuclear architecture in growing mouse oocytes. Mol Cell Endocrinol 234:11–17.